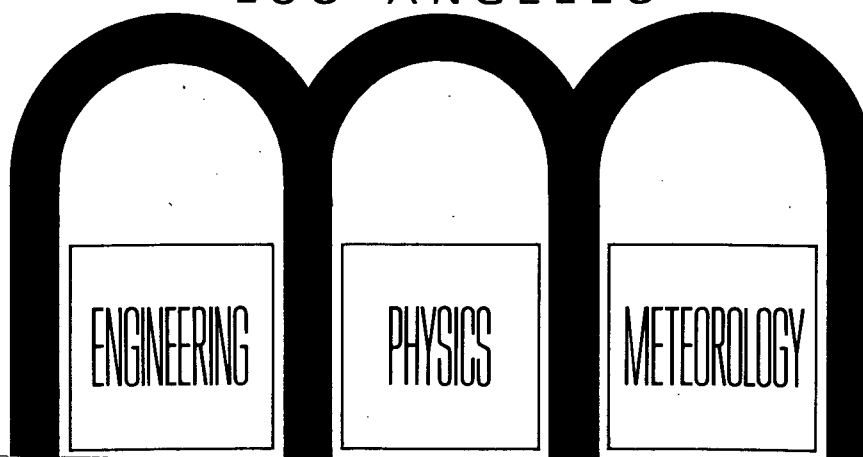


PLASMA PHYSICS GROUP



UNIVERSITY OF CALIFORNIA
LOS ANGELES



(NASA-CR-127387) STRUCTURE OF ION ACOUSTIC
SOLITONS AND SHOCK WAVES IN A TWO COMPONENT
PLASMA R.B. White, et al (California
Univ.) Sep. 1971 29 p

CSCL 20I

N72-27770

Unclas

G3/25 14133

**Structure of Ion Acoustic
Solitons and Shock Waves in a Two Component Plasma**

Roscoe B. White

Burton D. Fried

Ferdinand V. Coroniti

September, 1971

PPG-100

**Plasma Physics Group
Department of Physics
University of California
Los Angeles, California 90024**

**This work was partially supported by the Office of Naval Research,
Grant #N00014-69-A-0200-4023; the National Science Foundation, Grant
#GP-22817; the Atomic Energy Commission, Contract AT(04-3)-34, Project
#157; and the National Aeronautics and Space Administration, Contract
NGR-05-007-190 and NGR-05-007-116.**

Abstract

Time independent solitary waves and shocks are investigated in two component plasma using a fluid model and kinetic theory. It is found that very small concentrations of a light ion can drastically alter the structure, changing the potential maximum ϕ_m by an order of magnitude. For a fixed Mach number, a critical density ratio of light to heavy ions is found at which ϕ_m changes discontinuously from a value large enough to reflect the light ions to one which allows them to traverse the shock front and enter the downstream flow. The downstream oscillatory structure normally seen in a shock is completely quenched by dissipation due to light ion reflection at concentrations of 3 - 8% He in an A plasma for typical T_e/T_i and Mach number values.

I. Introduction

Electrostatic, ion-acoustic shock waves in the collisionless regime provide one of the simplest and most easily analyzed examples of collisionless shock waves in a plasma. In addition to their intrinsic interest on fundamental grounds, they are important also because high Mach number collisionless shock waves propagating across a magnetic field require an electrostatic subshock to provide sufficient dissipation.¹ The structure of such electrostatic shocks was treated by Moiseev and Sagdeev² with a simple model: a time-independent theory of cold (fluid) ions and isothermal electrons. Actually, this simple theory predicts only "solitons", i.e., pulse-like potential structures in which there is no net change, the potential profile, $\phi(z)$, being either periodic in z or else symmetric about its maximum point. Including additional physical effects (e.g., ion thermal motion, with a consequent reflection of some ions) results in a shock-like structure, with ϕ and the other physical variables undergoing a net change across the shock, but the simple Moiseev-Sagdeev theory continues to be valuable as a description of the leading portion of the shock front.

On physical grounds, it would be expected that the shock structure would be significantly affected by the presence of lighter ions, since these can be reflected by the potential even when the dominant (heavy ion) species suffers little or no reflection. We show here that very small concentrations of a light ion can drastically alter the shock or soliton structure, changing the height ϕ_m of the potential maximum by an order of magnitude. In fact, if $\alpha = N_2/N_1$ is the density ratio of light to heavy ions, there exists a critical value, α_c , depending principally on the mass ratio, $\mu = m_1/m_2$, and the shock Mach number, above which ϕ_m drops discontinuously from a value large enough to

reflect the light ions to one which allows them to traverse the shock front and enter the downstream flow. Equivalently, for given α , we find a new critical Mach number, $M_c(\alpha)$ for the transition from a small amplitude shock or soliton, which allows light ions to stream past it (in the shock rest frame) to a large amplitude which reflects all of the light ions. In fact, for a given concentration of light ions incident on the shock, α_i , there is a forbidden band of Mach numbers, $M_c(\alpha_i) < M < M_c(2\alpha_i)$, for which no steady state solution can exist.

These results follow very simply in the cold fluid approximation, as shown in section II. Moreover, thermal effects cause only quantitative changes, so long as T_i/T_e is not so large as to prevent shock or soliton solutions altogether. This is discussed in section III, where a Vlasov equation treatment is used for the light ions, the heavy ions being treated as either a cold fluid ($T_1 = 0$) or with a Vlasov treatment, assuming equal temperatures for light and heavy ions.

II. Cold Fluid Analysis

The essential features of the two species problem can be seen most clearly in the limit where both ion species are treated as cold fluids, with density n_j , flow velocity V_j , mass m_j , where ($j = 1, 2$) and $\mu = m_1/m_2 > 1$. From the conservation laws, we have in the shock rest frame

$$n_j V_j = N_j u$$

$$V_j^2 + 2e\phi/m = u^2$$

and hence

$$n_j = N_j (1 - 2e\phi/m_j u^2)^{-1/2}$$

where u is the shock velocity in the lab frame and N_j is the total density of

species j in the upstream region. (If the light ions are reflected by the shock, N_2 represents the sum of incident and reflected ions.) The electrons we treat as isothermal,

$$n_e = N \exp(e\phi/T_e) .$$

Expressing Poisson's equation

$$d^2\phi/dz^2 = 4\pi e(n_e - n_1 - n_2)$$

in terms of the dimensionless potential

$$\psi = 2e\phi/m_1 u^2$$

and using the electron Debye length

$$k_D^{-1} = (T_e/4\pi N e^2)^{1/2}$$

as a unit of length, we have

$$\begin{aligned} \psi'' &= (2/M^2) \{ \exp(M^2\psi/2) - (1-\alpha)(1-\psi)^{-1/2} - \alpha(1-\mu\psi)^{-1/2} \} \\ &\equiv - dV/d\psi \end{aligned}$$

where $\alpha_2 = N_2/N$ gives the total concentration of the light ion species. The function $V(\psi)$ is a simple extension of the Sagdeev potential; from it we can immediately deduce the qualitative features of the solutions, $\psi(z)$, by exploiting the analogy to particle motion in a potential well ($z \sim$ time, $\psi \sim$ particle coordinate, $V \sim$ potential energy). Choosing the constant of integration to make $V(0) = 0$, we have

$$\begin{aligned} V(\psi, M, \alpha) &= - 4/M^2 \{ M^{-2} [\exp(M^2\psi/2) - 1] + (1-\alpha) [(1-\psi)^{1/2} - 1] \\ &\quad + (\alpha/\mu) [(1-\mu\psi)^{1/2} - 1] \} . \end{aligned} \quad (1)$$

In Fig. 1, we show how $V(\psi)$ varies with Mach number M for given light ion concentration, α , and with α for given M , with mass ratio $\mu = m_1/m_2 = 5$. The

maximum potential, ψ_m , is given by the first non-zero root of $V(\psi)$. For small α or large M , this exceeds $1/\mu$, and so all of the light ions are reflected. However, the light ions do cause a modification in $V(\psi)$, namely the small cusp-like structure near $\psi = \mu^{-1}$. When a critical value of α is reached, this cusp crosses the ψ axis, resulting in a sharp drop of ψ_m to a value so small that the light ions are no longer reflected. [This continues to be the case as α increases, until a limit is reached at which the condition $(d^2V/d\psi^2)_{\psi=0} < 0$, required for the existence of soliton solutions, is violated. Since

$$(d^2V/d\psi^2)_{\psi=0} = -M^{-2}[M^2 - \mu\alpha - (1-\alpha)]$$

we must have $M^2 > 1 + (\mu-1)\alpha$, i.e., u must exceed the ion acoustic speed based on the reduced ion mass.]

The critical value of α for given M , or, equivalently, the critical Mach number, M_c , for given α is obtained from

$$V(\mu^{-1}, M_c, \alpha) = 0 \quad (2)$$

We can solve explicitly for α in terms of M and μ :

$$\alpha = [(\exp(M^2/2\mu) - 1)M^{-2} + p - 1]/p(p-1); \quad p = (1 - \mu^{-1})^{1/2} \quad (3)$$

which leads to the critical Mach number curves shown in Fig. 2. For $\mu \gg 1$, we have

$$\alpha \approx (M^2-1)/4\mu + (2M^4 + 3M^2 + 3)/48\mu^2 \quad (4)$$

or

$$M_c \approx (1 + 4\mu\alpha - 2/3\mu)^{1/2}$$

which explains the nearly straight-line shape of the curves in Fig. 2.³ If, for given M , we increase α from zero, the soliton structure develops a shoulder at $\psi = \mu^{-1}$, the amplitude, $\psi_m \approx 1$, being large enough to reflect the light ions. The point of reflection occurs where $\psi = \mu^{-1}$; there, the light ion density has

an integrable singularity, which manifests itself in the cusp in $V(\psi)$ at $\psi = \mu^{-1}$. As the light ion concentration increases, the density singularity becomes stronger and eventually, at a value of α given by (3), brings ψ_m down to a value just below μ^{-1} , at which point the light ions are no longer reflected.

In addition to the prediction of a critical Mach number (or light ion concentration), with ψ_m changing discontinuously as we cross the M^2 vs. α curve in Fig. 2, another discontinuity associated with this phenomenon appears when we consider the application to an experimental situation. This arises from the fact that in the upstream region we must distinguish two measures of light ion concentration. One is the quantity α used above, defined to be the total concentration, $\alpha = N_2/N$, where N_2 is the total density of light ions, not only those incident on the shock, but also those reflected, if any. The other measure, which we denote as α_1 , is defined as the density of incident light ions only. When there is light ion reflection, we have $\alpha = 2\alpha_1$; otherwise, $\alpha = \alpha_1$. Suppose, now, that the shock is propagating into a quiescent plasma, characterized by some value of α_1 . If M is below the critical value, $M_c(\alpha_1)$, then there is no reflection; $\alpha = \alpha_1$; and we have a small amplitude shock. If M is increased until it is infinitesimally larger than $M_c(\alpha_1)$, then the shock becomes large enough to reflect the light ions and we have $\alpha = 2\alpha_1$. However, M is now well below the critical Mach number, $M_c(2\alpha_1)$ corresponding to this larger value of α , implying that the light ions are not reflected. We conclude that there is no steady state solution for M in the range $M_c(\alpha_1) < M < M_c(2\alpha_1)$. Once M exceeds $M_c(2\alpha_1)$ we have again a self consistent solution, with reflected light ions. The situation is summarized in Fig. 3 which shows the forbidden region of Mach numbers for the case $\mu = 10$.

In a sense, this range of forbidden Mach numbers makes the discontinuous change in ψ_m which occurs on crossing the M_c^2 vs. α curve (Fig. 2) less

surprising. If we consider the incident light ion concentration, α_1 , to be the physically relevant parameter, then it follows that for α_1 fixed, ψ_m increases continuously from 0 to μ^{-1} as M goes from 1 to $M_c(\alpha_1)$. Beyond that point, no further continuous change in M is possible until we get to $M_c(2\alpha_1)$. There we will, indeed, have ψ_m of order 1, but at least this finite change in ψ_m is associated with a finite change in M .

It might be thought that these discontinuous features of the problem are a consequence of our neglect of thermal effects, since a distribution in ion velocity would remove the singularity in density associated with the reflection of all light ions at a single location. In the following section, we show that inclusion of thermal effects for the light ions rounds and diminishes the cusp at $\psi = 1/\mu$, so that a higher concentration of light ions is required for the transition from large to small shock amplitudes, for given Mach number. However, the transition, when it occurs, is still an abrupt one and there continues to be a band of forbidden Mach numbers. Of course, as T_2/T_e increases, the whole effect washes out, just as the shock itself does when T_1/T_e is not small.

III. Vlasov Analysis

As before, we work in the shock rest frame. Initially, we continue to use a cold fluid treatment for the heavy ions, since their thermal velocities are typically small compared to the shock velocity, u . However, the light ion thermal velocities can be comparable to u , so we treat them with a distribution function, $f(v, z)$, which satisfies the Vlasov equation.

Since the problem is time-independent, the ion equations of motion again reduce to conservation laws:

$$n_1 v_1 = N_1 u$$

$$v_1^2 + (2e\phi/m_1) = u^2$$

$$f(v, z) = F[(v^2 + 2e\phi(z)/m_2)^{1/2}] \quad (5)$$

where n_1, v_1 are the density and mean velocity of the heavy ions; f is the light ion distribution function; ϕ is the electrostatic potential, chosen to be zero at $z = -\infty$, where the heavy ion density is N_1 ; and $F(v)$ gives the light ion distribution function at $z = -\infty$,

$$F(v) = f(v, -\infty)$$

normalized⁴, so that

$$\int_0^\infty dv F(v) = 1$$

From f , we find the light ion density at any point, z , from

$$n_2(z) = N_{2i} \int_{-\infty}^\infty f(v, z) dv \quad (6)$$

where N_{2i} is the density of light ions incident on the shock, i.e., the density of all light ions at $z = -\infty$ which have not been reflected at the shock. For the electrons, we assume isothermal equilibrium

$$n_e = N \exp(e\phi/T_e) \quad (7)$$

Charge neutrality at $z = -\infty$ requires

$$N = N_1 + N_{2i}(1+q) = N_1 + N_2 \quad (8)$$

where q is the fraction of incident light ions which are reflected by the shock:

$$q = \int_{-\infty}^0 dv F(v)$$

For the light ions, we assume, far upstream, essentially a Maxwellian distribution

plus that portion of the incident ions which are reflected by the shock, i.e., all those with incident velocity

$$v \leq v_m = (2e\phi_m/m_2)^{1/2} \quad (10)$$

where ϕ_m is the maximum of ϕ . If we were treating a time dependent problem, it would be appropriate to assume a full Maxwellian upstream. However, in the context of a steady state problem, ions with $v < 0$ in the upstream region can have only two sources:

1. Those ions which had, initially, a positive velocity and have been reflected by the shock front.
2. Those ions which have come through the shock from the downstream region, and hence have a velocity not less than $[2e(\phi_m - \phi)/m_2]^{1/2}$.

In the present discussion we shall neglect this second possibility, i.e., we assume that far downstream there are only light ions with $v > 0$ which have come through the shock from the upstream region.⁵ Then $F(v)$ is given by

$$F(v) = \frac{c_2}{a_2 \pi^{1/2}} \exp[-(v-u)^2/a_2^2] \quad (11)$$

and

$$F(v) = F(-v) \quad -v_m < v < 0$$

where (5) requires

$$\frac{c_2}{\pi^{1/2}} \int_{-u/a_2}^{\infty} dw e^{-w^2} = \frac{c_2}{2} [1 + \operatorname{erf} \gamma] = 1 \quad (12)$$

where $\gamma = u/a_2$. For cold ions ($\gamma \rightarrow \infty$), $C_2 \rightarrow 1$. The fraction of reflected ions, q , which appears in (8) is given by

$$q = \frac{c_1}{\pi^{1/2}} \int_{(u-v_m)/a_2}^{u/a_2} dw e^{-w^2} = (C_2/2) \{ \operatorname{erf} \gamma - \operatorname{erf} [\gamma - \gamma(\mu\psi_n)^{1/2}] \} \quad (13)$$

For the light ion density (6) we then have from (5) and (11)

$$\frac{n_2(z)}{N_{21}} = \int_0^{\infty} dv F((v^2 + \chi^2)^{1/2}) + \int_0^{\chi_m} dv F((v^2 + \chi^2)^{1/2})$$

where

$$\chi = [2e\phi(z)/m_2]^{1/2} = u(\mu\psi)^{1/2}$$

is the velocity which a light ion has at $z = -\infty$ if it gets reflected by the shock potential at the point z . It is convenient to introduce

$$\hat{v} = (v^2 + \chi^2)^{1/2}$$

which is the velocity, at $z = -\infty$, of a light ion which reaches the point z with velocity v . Then

$$\frac{n_2}{N_{21}} = \int_{\chi}^{\infty} d\hat{v} \hat{v} F(\hat{v}) [\hat{v}^2 - \chi^2]^{-1/2} + \int_{\chi}^{\chi_m} d\hat{v} \hat{v} F(\hat{v}) [\hat{v}^2 - \chi^2]^{-1/2} \quad (14)$$

where

$$\chi_m = u(\mu\psi_m)^{1/2}.$$

We can write (14) as

$$n_2/N_2 = -\partial V_2 / \partial \chi^2 \quad (15)$$

where

$$V_2 = 2 \left\{ \int_{\chi}^{\infty} d\hat{v} \hat{v} F(\hat{v}) [\hat{v}^2 - \chi^2]^{1/2} + \int_{\chi}^{\chi_m} d\hat{v} \hat{v} F(\hat{v}) [\hat{v}^2 - \chi^2]^{1/2} \right\}. \quad (16)$$

In terms of the dimensionless potential

$$\psi = 2e\phi/m_1 u^2 \quad (17)$$

we have for the first term in V_2

$$\int_{\chi}^{\infty} d\hat{v} \hat{v} F(\hat{v}) [\hat{v}^2 - \chi^2]^{1/2} = (C_2/a_2^2 \pi^{1/2}) \int_{u(\mu\psi)^{1/2}}^{\infty} d\hat{v} \hat{v} \exp[-(\hat{v}-u)^2/a_2^2] [\hat{v}^2 - \mu u^2 \psi]^{1/2}$$

$$= C_2 \pi^{-1/2} \gamma u^2 \int_{(\mu\psi)^{1/2}}^{\infty} dw \cdot w (w^2 - \mu\psi)^{1/2} \exp[-\gamma^2 (w-1)^2]$$

where $\gamma = u/a_2$. Making similar changes of variables in the second term, we find

$$V_2(\psi) = 2u^2 U_{\mu}(\psi)$$

with

$$U_{\mu}(\psi) = \int_{(\mu\psi)^{1/2}}^{\infty} dw G_{\mu}(w) + \int_{(\mu\psi)^{1/2}}^{(\mu\psi_m)^{1/2}} dw G_{\mu}(w) \quad (18)$$

$$G_{\mu}(w) = c_2 \pi^{-1/2} \gamma w (w^2 - \mu\psi)^{1/2} \exp[-\gamma^2 (w-1)^2] \quad (19)$$

The first term in (18) corresponds to incident light ions, the second term to reflected ones.

Since $n_2/N_{2i} = (n_2/N_2)(1+q) = \alpha(1+q)$ and

$$\frac{n_2}{N_{2i}} = - \frac{\partial V}{\partial \chi^2} = - \frac{1}{\mu u^2} \frac{dV}{d\psi} = - \frac{2}{\mu} U_{\mu}^1(\psi) \quad (20)$$

we see that $U_{\mu}(\psi)/(1+q)$ replaces the term $(1-\mu\psi)^{1/2}$ in the expression (1) for $V(\psi)$. In fact, in the limit $a_2 \rightarrow 0$ we have, for $\mu\psi < 1$,

$$C_2 \rightarrow 1 \quad G(w) \rightarrow \delta(w-1) (1-\mu\psi)^{1/2}$$

$$U_{\mu}(\psi) \rightarrow \begin{cases} (1-\mu\psi)^{1/2} & \mu\psi < 1 \\ 2(1-\mu\psi)^{1/2} & \mu\psi > 1 \end{cases}$$

$$q \rightarrow \begin{cases} 0 & \mu\psi_m < 1 \\ 1 & \mu\psi_m > 1 \end{cases}$$

so $U_{\mu}(\psi)/(1+q) \rightarrow (1-\mu\psi)^{1/2}$.

Adding the other terms representing electrons and heavy ions, we have for the Sagdeev potential

$$V(\psi) = -4M^{-2}\{M^{-2}[\exp(M^2\psi/2)-1] + (1-\alpha)[(1-\psi)^{1/2} - 1] + \frac{\alpha}{\mu} U_{\mu}(\psi)/(1+q)\} \quad (21)$$

where the parameters of the problem are Mach number, M ; total upstream light ion concentration, α ; mass ratio, $\mu = m_1/m_2 > 1$; and the light ion/electron temperature ratio T_2/T_e . The quantity, γ , which is involved in C_1 , q , and U , can be expressed in terms of these:

$$\gamma = M(T_e/2\mu T_2)^{1/2} \quad (22)$$

In contrast to the cold fluid case ($\gamma \rightarrow \infty$), note that ψ_m enters also as a parameter, and must be determined self-consistently with (21), ψ_m being the largest root of (21) on the interval $0 \leq \psi \leq 1$.

Representative plots of $V(\psi)$ for varying values of $\theta = T_e/T_2$ are shown in Fig. 4. For very large θ , the cusp near $\psi = 1/\mu$ is rounded, due to the spread in reflection points of the light ions. For smaller θ , it is reduced in amplitude, and below a value of θ_c of order 100 the effect disappears entirely. For $\theta \geq \theta_c$, the transition from small to large amplitude shocks still occurs, but for given concentration the critical Mach number is larger. This is shown in Figs. 5, 6, where plots of M_c vs. α are given for various values of θ .

A plot of Mach number versus amplitude for fixed θ , n_2/n_e is shown in Fig. 7. Near point A on the large amplitude shock segment, the light ion cusp is approaching very close to zero. The shock then possesses a very long foot in which the reflected light ions have a very low velocity in the shock frame. One would thus expect the onset of the two stream instability, and therefore the forbidden region in Fig. 7 (for laminar shocks) might be bridged by a turbulent region.

It is easy to consider the thermal effects associated with the heavy ions, which can become important at large Mach numbers. When the heavy ions are cold, $V(\psi)$ has a cusp at $\psi = 1$, again due to the singularity in density at the reflection point. Thermal effects remove this singularity, just as in the case of the light ions, and cause a smearing of the cusp in $V(\psi)$. If T_1/T_e is too large, $V(\psi)$ may remain negative for all ψ , and no steady shock or soliton solution is possible. As pointed out by Moiseev and Sagdeev,² a similar effect occurs even at $T_1 = 0$ when M gets large, resulting in an upper limit: $M \leq M^0 = 1.6$. Segre and Bardotti⁶ have calculated the reduction in M^0 as T_1/T_e increases for the single species case, and we have included curves for M^0 vs. α in Figs. 5, 6 for several values of T/T_e , with $T_1 = T_2 = T$. Formally, the Sagdeev potential for $T_1 \neq 0$ is obtained by using $U_1(\psi)/(1+q_1)$ in place of $(1-\psi)^{1/2}$ in (22), where U_1 is given by (18) with $\mu = 1$ and q_1 is given by (13), again with $\mu = 1$.

As described by Bardotti and Segre, the reflection of ions from the potential also provides a dissipative mechanism, and in fact leads to a shock rather than a solitary wave even in the absence of other dissipative effects. The addition of a light ion further enhances this effect in two ways. Firstly, the light ions themselves are totally reflected in the large amplitude shock region. Secondly, for fixed Mach number the addition of light ions slightly increases the amplitude of the shock, causing the increased reflection of heavy ions. This effect can be simply examined by calculating the Sagdeev potential for the downstream state, given by removing the reflected ion terms from the upstream potential. Examples of the potential for upstream and downstream states are shown in Fig. 8. The result obtained is that a small addition of light ions can entirely quench the downstream oscillatory structure. This effect depends very sensitively on the ratio T_e/T_1 , the light ion concentration,

and on the Mach number, but in general complete quenching is observed for only 5% He concentration in an A plasma.⁷ It has been pointed out by Forslund and Shonk⁸ that numerical simulation studies of acoustic shock waves indicate a flattening of the electron distribution function occurs, with a resulting change in the equation of state from the isothermal law which we have used. Specifically, the electron density is assumed to have the form

$$n_e = N \{ (2\pi)^{-1/2} M \psi^{1/2} + \exp(\psi M^2/2) \cdot \text{erfc}[(\psi/2)^{1/2} M] \}$$

where erfc is the complement of the error function. This density corresponds to a distribution in velocity which is constant for $|v/u| \leq (m_1/m_e)^{1/2} \psi^{1/2}$, and given by adiabatic displacement of a Maxwellian from a point where $\psi = 0$ for $(v/u) > (m_1/m_e)^{1/2} \psi^{1/2}$. The authors refer to this distribution as maximum density electron trapping, although the electron density is less than that given by the Boltzmann law. We have repeated our calculations using this modified equation of state and find that the numerical results concerning transition from small to large amplitude shocks are not greatly changed. This is to be expected, as the cusp due to the light ions appears for very small ψ , whereas the two electron equations of state differ for large ψ . The range of Mach numbers for which the theory is valid is increased, M^0 in the case of a cold single ion species changing from 1.6 to 3.1. Most important, the ion reflection from the shock is significantly changed for low θ , and the quenching of downstream oscillations is very sensitive to this. Figure 9 shows the quenching of the downstream oscillations for a few representative Mach numbers and typical laboratory values of θ , using both electron equations of state. Note that for these values of θ there is no transition to a small amplitude shock.

Conclusion

Two important effects are caused by the addition of a small light ion concentration in a heavy ion plasma. In the range of $T_e/T_i \gg 1$ (for a He-A plasma $T_e/T_i > 70$ is sufficient) there exists a critical Mach number, depending on n_2/n_1 , at which the potential maximum changes discontinuously. This discontinuous change results in a band of Mach numbers in which no steady state laminar solution exists. This range of θ is unfortunately not yet experimentally accessible and the transition from small to large amplitude shocks has not been observed. In numerical simulation experiments carried out by Forslund and Morse,⁹ with values of $\theta = 400$, a small amplitude shock with almost no light ion reflection forms, followed by a region of turbulent heating which raises the ion temperature into the large amplitude shock region, after which a large amplitude shock forms which sweeps up all the light ions. The entire system is of course not time independent, the two shocks having very different Mach numbers, but insofar as each individual shock front is time independent, we identify them as the large and small amplitude shocks of the present theory. The second effect is the quenching of the downstream oscillatory structure in the shock, which is present to a greater or lesser degree for all values of θ . This quenching has been experimentally observed and the preliminary experiments agree with the results of Fig. 9, the indicated electron trapping being intermediate between the Boltzmann result and the uniform density trapping result. Final experimental results will be reported in a separate publication.

Acknowledgment

The authors would like to express their indebtedness to Professors Charles F. Kennel and Roald Z. Sagdeev for suggestions which initiated theoretical research in multi-ion plasmas.

References

1. A. E. Robson, Collision-free Shocks in the Laboratory and Space, Proceedings of a Study Group held at the European Space Research Institute, Frascasti, ESRO SP-51, December, 1969.
2. S. S. Moiseev and R. Z. Sagdeev, Plasma Physics 5, 43 (1963).
3. The upper curve in Fig. 2, labeled M^0 , is a limit above which the Sagdeev potential fails to intercept zero, and no bounded solution to the problem exists. In the limit $n_2 = 0$, $M^0 \sim 1.6$.
4. We choose this normalize for F to facilitate comparison with experimental results, where the most convenient parameter characterizing the light ion concentration is their fraction in the unperturbed upstream plasma. See also the discussion preceding Eq. (11).
5. In fact this turns out to be an academic point; for physicall interesting parameters the difference is negligible.
6. G. Bardotti and S. E. Segre, Plasma Physics 12, 247 (1970).
7. K. R. MacKenzie and R. J. Taylor, Bull. Am. Phys. Soc. 15, 1409 (1970).
8. D. W. Forslund and C. R. Shonk, Phys. Rev. Letters 25, 1699 (1970).
9. D. Forslund and R. Morse, private communication.

Figure Captions

- Fig. 1. Sagdeev Potential, $V(\psi)$, in the cold ion limit, for $m_1/m_2 = 5$. In a), the light ion concentration, $\alpha = n_2/n_e$, is held fixed at 1% while the Mach number M is varied. In b), M is fixed at 1.2 and n_2/n_e is varied.
- Fig. 2. Critical Mach number, M_c , as a function of light ion concentration for $\theta = T_e/T_i = \infty$, $m_1/m_2 = 5$.
- Fig. 3. Critical Mach number as a function of incident light ion density, α_i , for $\theta = 100$, $m_1/m_2 = 10$.
- Fig. 4. Thermal broadening of cusp in pseudopotential as a function of $\theta = T_e/T_i$ for fixed M and α .
- Fig. 5. Critical Mach number M_c as a function of $\theta = T_e/T_i$ for $\mu = m_1/m_2 = 5$.
- Fig. 6. Critical Mach number, M_c , as a function of $\theta = T_e/T_i$ for $\mu = m_1/m_2 = 10$.
- Fig. 7. Forbidden region in amplitude and Mach number for $\theta = 100$, $n_{2i}/n_e = 2\%$.
- Fig. 8. The Sagdeev potential for upstream and downstream states for various θ , n_2/n_e , with $M = 1.25$.
- Fig. 9. Quenching of downstream oscillations by light ion addition (He in A) with two choices for the electron equation of state.

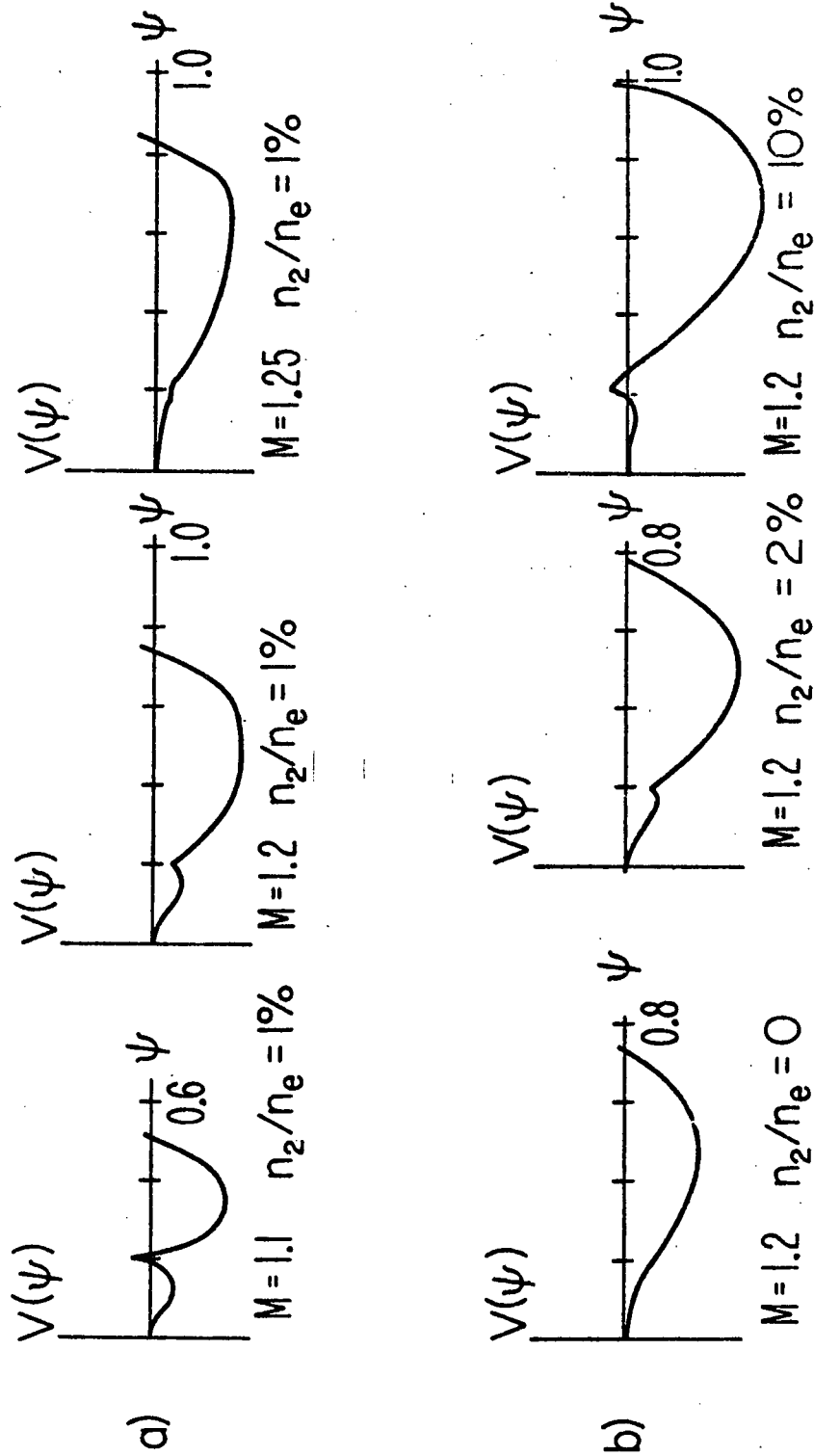


Fig. 1. Sagdeev Potential, $V(\psi)$, in the cold ion limit, for $m_1/m_2 = 5$. In a), the light ion concentration, $\alpha = n_2/n_e$, is held fixed at 1% while the Mach number M is varied. In b), M is fixed at 1.2 and n_2/n_e is varied.

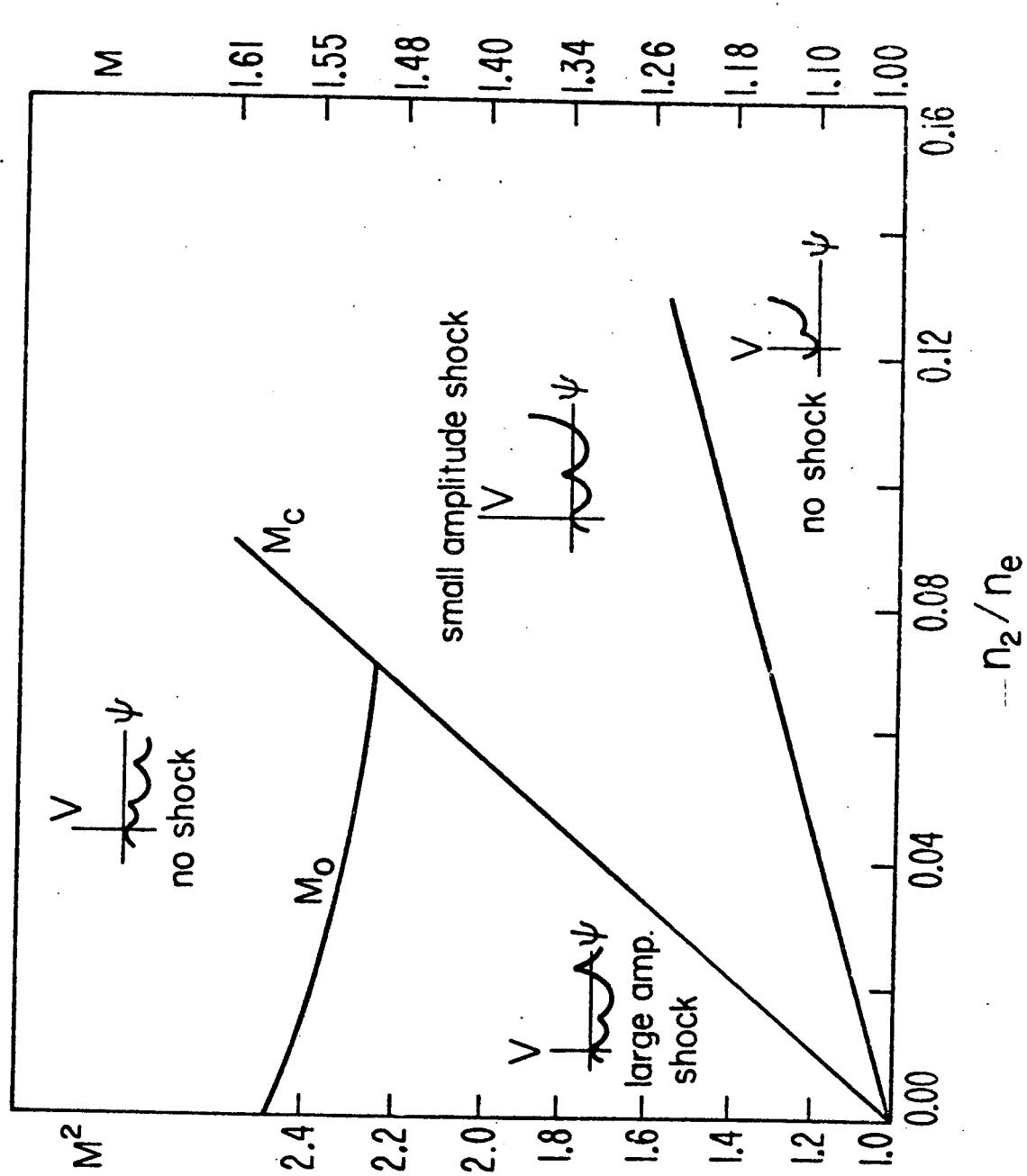


Fig. 2. Critical Mach number, M_c , as a function of light ion concentration for $\theta = T_e/T_i = \infty$, $m_1/m_2 = 5$.

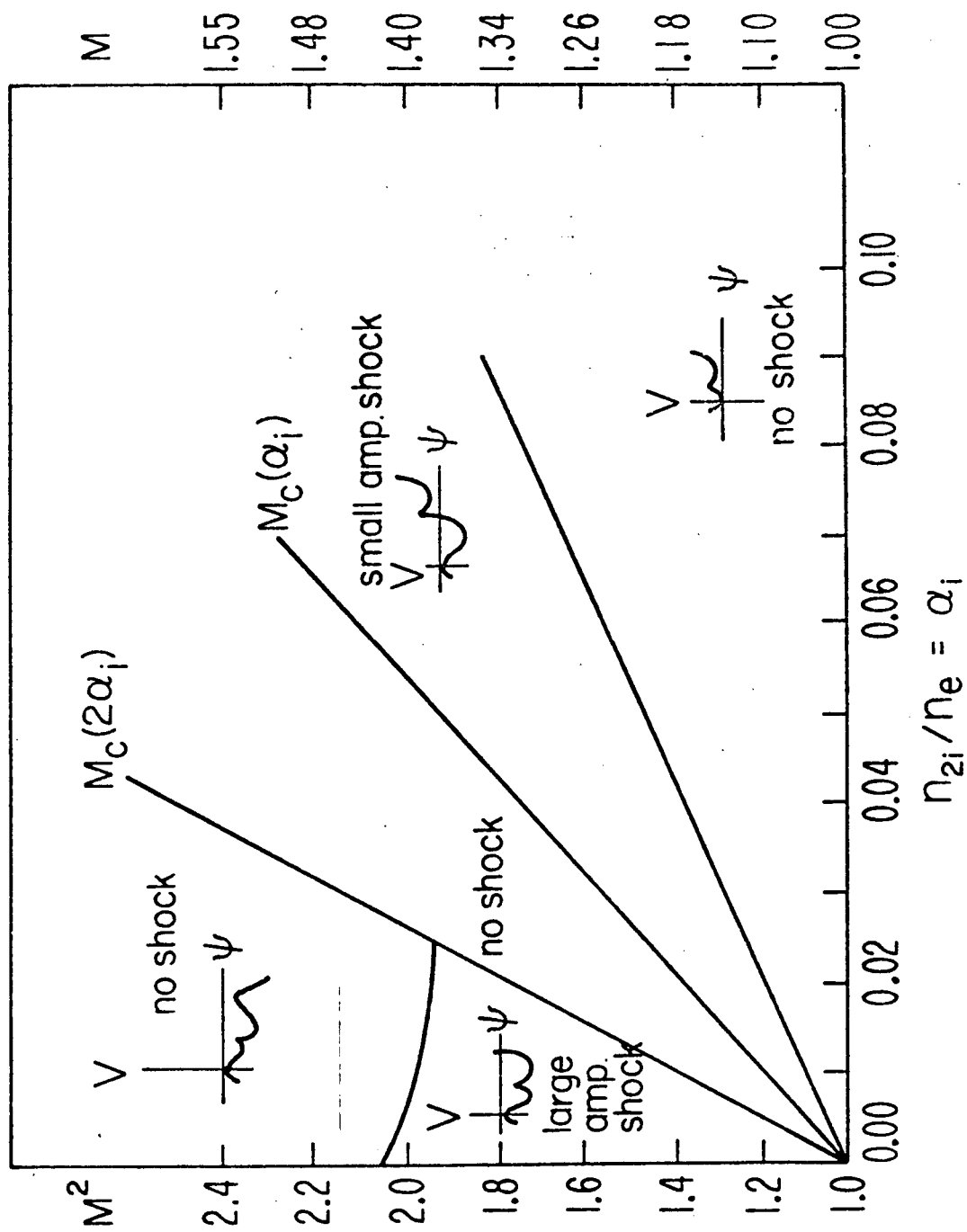


Fig. 3. Critical Mach number as a function of incident light ion density, α_i , for $\theta = 100$, $m_1/m_2 = 10$.

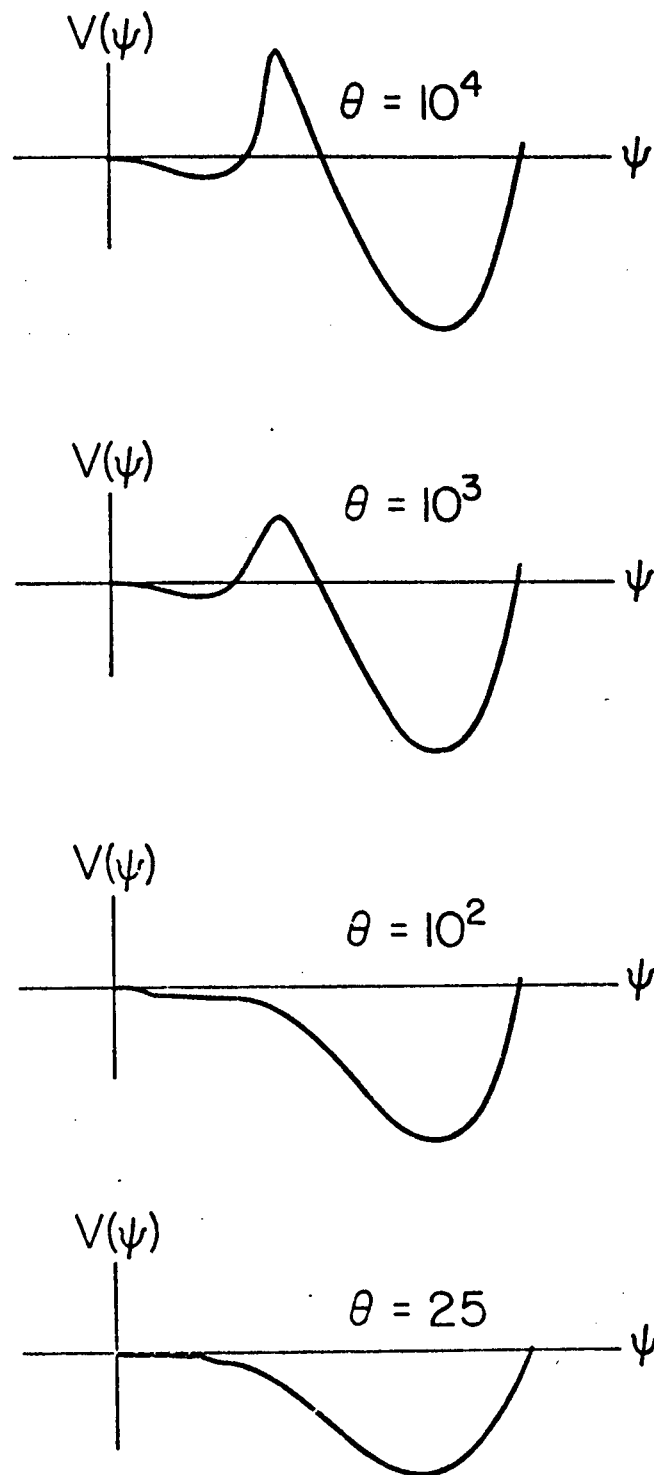


Fig. 4. Thermal broadening of cusp in pseudopotential as a function of $\theta = T_e/T_i$ for fixed M and α .

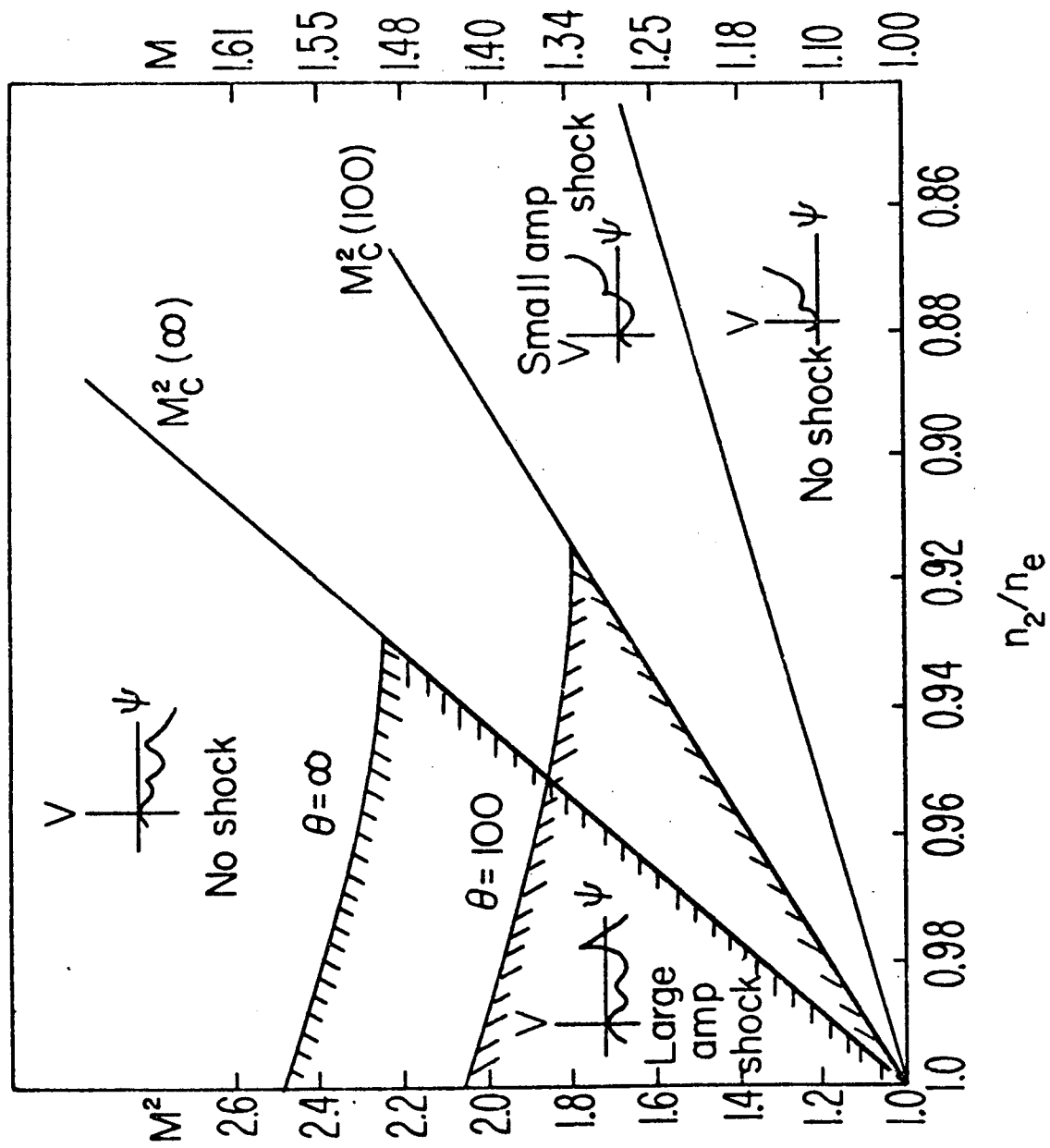


Fig. 5. Critical Mach number M_c as a function of $\theta = T_e/T_i$ for $\mu = m_1/m_2 = 5$.

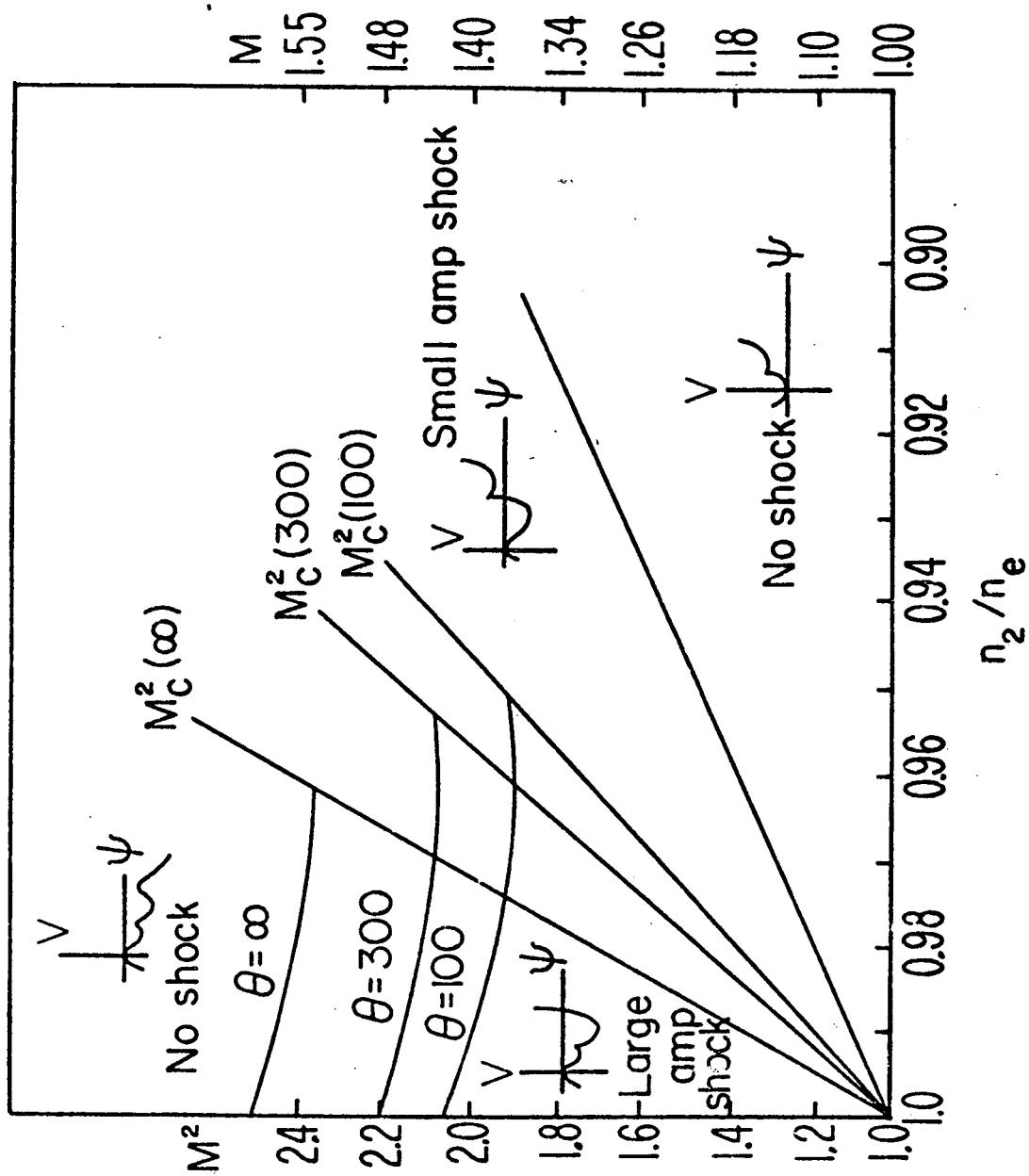


Fig. 6. Critical Mach number, M_c , as a function of $\theta = T_e/T_i$ for $\mu = m_1/m_2 = 10$.

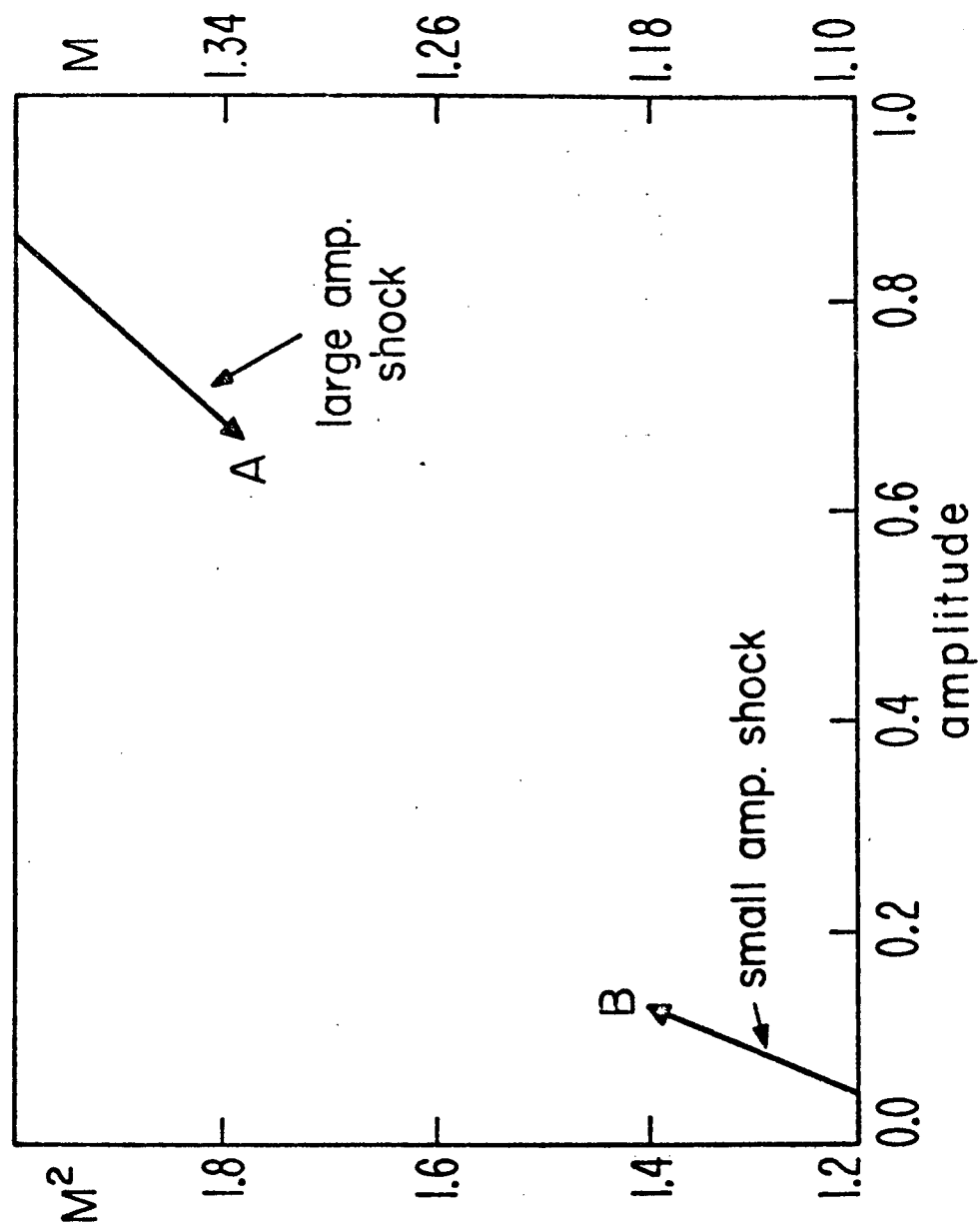


Fig. 7. Forbidden region in amplitude and Mach number for $\theta = 100$, $n_{2i}/n_e = 2\%$.

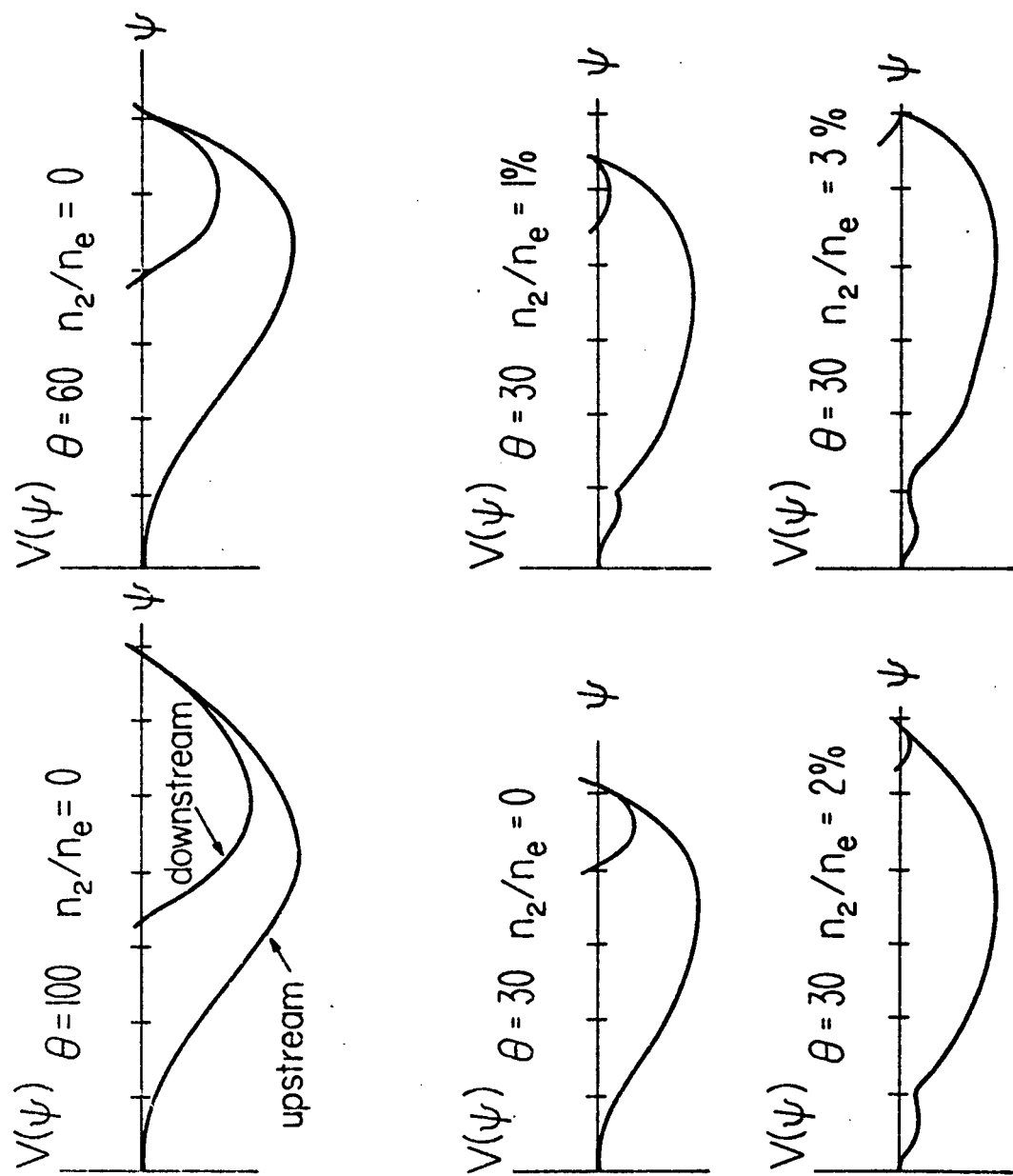


Fig. 8. The Sagdeev potential for upstream and downstream states for various θ , n_2/n_e , with $M = 1.25$.

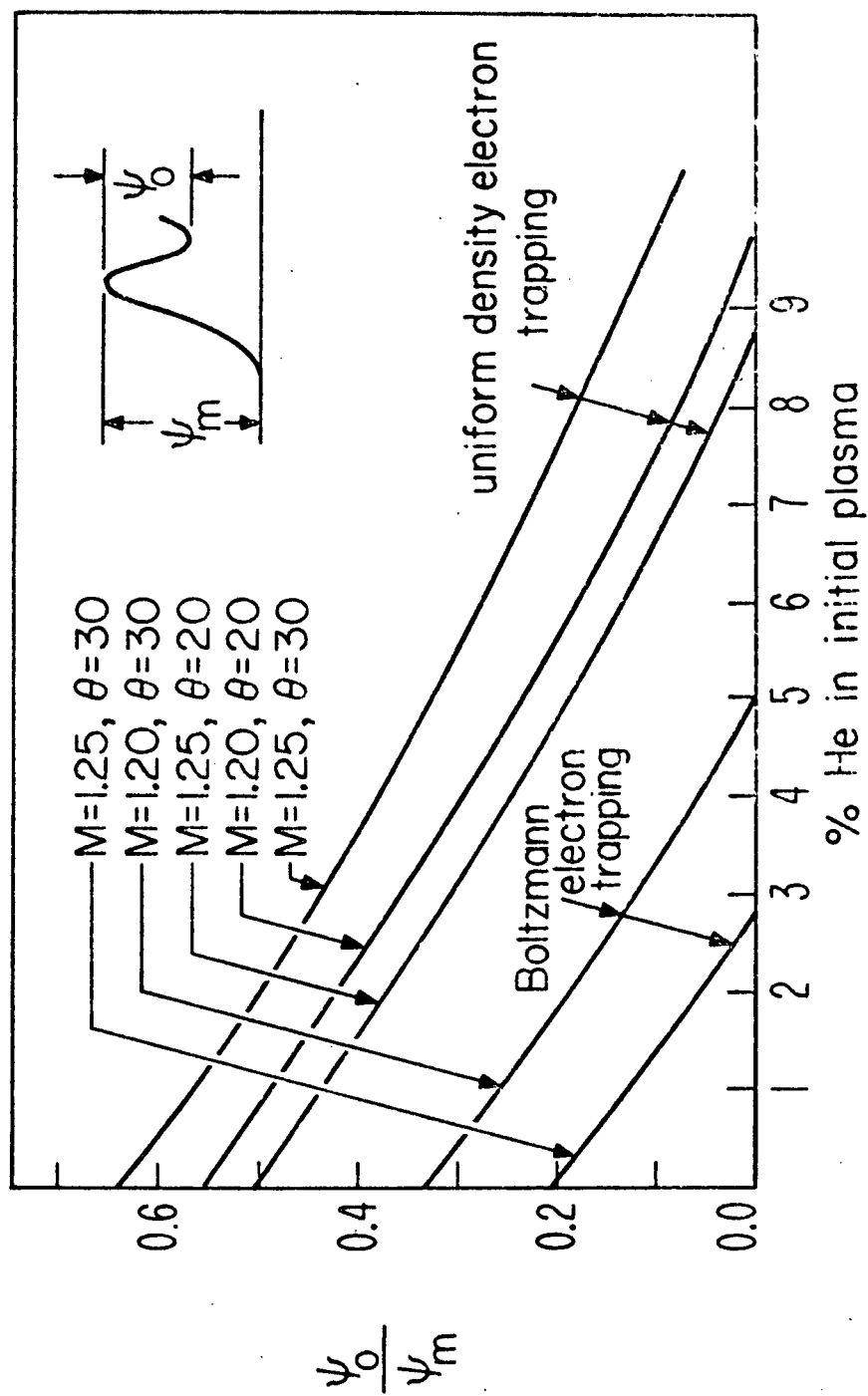


Fig. 9. Quenching of downstream oscillations by light ion addition (He in A) with two choices for the electron equation of state.

- R-1 "Propagation of Ion Acoustic Waves Along Cylindrical Plasma Columns", A.Y. Wong (July 1965)
- R-2 "Stability Limits for Longitudinal Waves in Ion Beam-Plasma Interaction", B.D. Fried and A.Y. Wong (August 1965)
- R-3 "The Kinetic Equation for an Unstable Plasma in Parallel Electric and Magnetic Fields", B.D. Fried and S.L. Ossakow (Nov. 1965)
- R-4 "Low-Frequency Spatial Response of a Collisional Electron Plasma", B.D. Fried, A.N. Kaufman and D.L. Sachs (Aug. 1965)
- R-5 "Effects of Collisions on Electrostatic Ion Cyclotron Waves", A.Y. Wong, O. Judd and F. Hui (Dec. 1965)
- R-6 "Interaction Between Ion Beams and Plasmas", R. Rowberg, A.Y. Wong and J.M. Sellen (April 1966)
- R-7 "Observation of Cyclotron Echoes from a Highly Ionized Plasma", D.E. Kaplan and R.M. Hill (May 1966)
- R-8 "Excitation and Damping of Drift Waves", A.Y. Wong and R. Rowberg (July 1966)
- R-9 "The Guiding Center Approximation in Lowest Order", Alfredo Banos, Jr. (Sept. 1966)
- R-10 "Plasma Streaming into a Magnetic Field", S.L. Ossakow (Nov. 1966)
- R-11 "Cooperative Effects in Plasma Echo Phenomena", A.Y. Wong (March 1967)
- R-12 "A Quantum Mechanical Study of the Electron Gas Via the Test Particle Method", M.E. Rensink (March 1967)
- R-13 "Linear and Nonlinear Theory of Grid Excitation of Low Frequency Waves in a Plasma", G.L. Johnston (April 1967)
- R-14 "The Expansion and Diffusion of an Isolated Plasma Column", J. Hyman (May 1967)
- R-15 "Two-pole Approximation for the Plasma Dispersion Function", B.D. Fried, C.L. Hedrick and J. McCune (August 1967)
- R-16 "Experimental Investigation of Electron Runaway Phenomena", J.S. DeGroot (August 1967)
- R-17 "Parametric Coupling Between Drift Waves", F. Hui, R. Rowberg and A.Y. Wong (Oct. 1967)
- R-18 "Cyclotron Echoes from Doppler Effects", A.Y. Wong (March 1968)
- R-19 "Ion Wave Echoes", D.R. Baker, N.R. Ahren and A.Y. Wong (Nov. 1967)
- R-20 "Cyclotron Echoes in Plasmas", O. Judd, Thesis (March 1968)
- R-21 "Test Particle Theory for Quantum Plasmas", M.E. Rensink (Oct. 1967)
- R-22 "Artificial Van Allen Belt", Charles F. Kennel (Nov. 1967)
- R-23 "Landau Damping of Ion Acoustic Waves in a Cesium Plasma with Variable Electron-Ion Temperature Ratio, K.B. Rajangam (Oct. 1967)
- R-24 "The Inhomogeneous Two-Stream Instability", G. Knorr (Sept. 1967)
- R-25 "Magnetic Turbulence in Shocks", C.F. Kennel and H.E. Petschek (Dec. 1967)
- R-26 "Small Amplitude in High Beta Plasmas", V. Formisano and C. Kennel (Feb. 1968)
- R-27 "Low Beta Plasma Penetration Across a Magnetic Field", B.D. Fried and S. Ossakow (March 1968)
- R-28 "Annual Status Report", Feb. 1, 1967-Jan. 31, 1968, Principal Investigators A. Banos, Jr., B.D. Fried, C.F. Kennel

- R-29 "The Theorist's Magnetosphere", C. Kennel (April 1968)
- R-30 "Electromagnetic Pitch Angle Instabilities in Space", C.F. Kennel and F.L. Scarf (April 1968)
- R-31 "Electromagnetic Echoes in Collisionless Plasmas", A.Y. Wong (April 1968)
- R-32 "Parametric Excitation of Drift Waves in a Resistive Plasma", G. Weyl and M. Goldman (June 1968)
- R-33 "Parametric Excitation from Thermal Fluctuations at Plasma Drift Wave Frequencies", A.Y. Wong, M.V. Goldman, F. Hai, R. Rowberg (May 1968)
- R-34 "Current Decay in a Streaming Plasma Due to Weak Turbulence", S.L. Ossakow and B.D. Fried (June 1968)
- R-35 "Temperature Gradient Instabilities in Axisymmetric Systems", C.S. Liu (August 1968)
- R-36 "Electron Cyclotron Echo Phenomena in a Hot Collisionless Plasma", O. Judd (August 1968)
- R-37 "Transverse Plasma Wave Echoes", B.D. Fried and Craig Olson (Oct. 1968)
- R-38 "Low Frequency Interchange Instabilities of the Ring Current Belt", C.S. Liu (Jan. 1969)
- R-39 "Drift Waves in the Linear Regime", R.E. Rowberg and A.Y. Wong (Feb. 1969)
- R-40 "Parametric Mode-Mode Coupling Between Drift Waves in Plasmas", F. Hai and A.Y. Wong (Jan. 1969)
- R-41 "Nonlinear Oscillatory Phenomena with Drift Waves in Plasmas", F. Hai and A.Y. Wong (Sept. 1960)
- R-42 "Ion-Burst Excited by a Grid in a Plasma", H. Ikezi and R.J. Taylor (Feb. 1969)
- R-43 "Measurements of Diffusion in Velocity Space from Ion-Ion Collisions", A. Wong and D. Baker (March 1969)
- R-44 "Nonlinear Excitation in the Ionosphere", A.Y. Wong (March 1969)
- R-45 "Observation of First-Order Ion Energy Distribution in Ion Acoustic Waves, H. Ikezi and R. Taylor (March 1969)
- R-46 "A New Representative for the Conductivity Tensor of a Collisionless Plasma in a Magnetic Field", B.D. Fried and C. Hedrick (March 1969)
- R-47 "Direct Measurements of Linear Growth Rates and Nonlinear Saturation Coefficients", F. Hai (April 1969)
- R-48 "Electron Precipitation Pulsations", F. Coroniti and C.F. Kennel (April 1969)
- R-49 "Auroral Micropulsation Instability", F. Coroniti and C.F. Kennel (May 1969)
- R-50 "Effect of Folker-Plank Collisions on Plasma Wave Echoes", G. Johnston (June 1969)
- R-51 "Linear and Nonlinear Theory of Grid Excitation of Low Frequency Waves in a Plasma", G. Johnston (July 1969)
- R-52 "Theory of Stability of Large Amplitude Periodic (BGK) Waves in Collisionless Plasmas", M.V. Goldman (June 1969)
- R-53 "Observation of Strong Ion Wave-Wave Interaction", R. Taylor and H. Ikezi (August 1969)
- R-55 "Optical Mixing in a Magnetoactive Plasma", G. Weyl (August 1969)
- R-56 "Trapped Particles and Echoes", A.Y. Wong and R. Taylor (Oct. 1969)
- R-57 "Formation and Interaction of Ion-Acoustic Solitons", H. Ikezi, R.J. Taylor and D.R. Baker (July 1970)

- R-58 "Observation of Collisionless Electrostatic Shocks", R. Taylor, D. Baker and H. Ikezi (Dec. 1969)
- R-59 "Turbulent Loss of Ring Current Protons", J.M. Cornwall, F.V. Coroniti and R.M. Thorne (Jan. 1970)
- R-60 "Efficient Modulation Coupling Between Electron and Ion Resonances in Magnetoactive Plasmas", A. Wong, D.R. Baker, N. Booth (Dec. 1969)
- R-61 "Interaction of Quasi-Transverse and Quasi-Longitudinal Waves in an Inhomogeneous Vlasov Plasma", C.L. Hedrick (Jan. 1970)
- R-62 "Observation of Strong Ion-Acoustic Wave-Interaction", R.J. Taylor and H. Ikezi (Jan. 1970)
- R-63 "Perturbed Ion Distributions in Ion-Waves and Echoes", H. Ikezi and R. Taylor (Jan. 1970)
- R-64 "Propagation of Ion Cyclotron Harmonic Wave", E.R. Ault and H. Ikezi (Nov. 1970)
- R-65 "The Analytic and Asymptotic Properties of the Plasma Dispersion Function", A. Banos, Jr. and G. Johnston (Feb. 1970)
- R-66 "Effect of Ion-Ion Collision and Ion Wave Turbulence on the Ion Wave Echo", Dan Baker (June 1970)
- R-67 "Dispersion Discontinuities of Strong Collisionless Shocks", F.V. Coroniti (March 1970)
- R-68 "An Ion Cyclotron Instability", E.S. Weibel (April 1970)
- R-69 "Turbulence Structure of Finite-Beta Perpendicular Fast Shocks", F.V. Coroniti (April 1970)
- R-70 "Steepening of Ion Acoustic Waves and Formation of Collisionless Electrostatic Shocks", R. Taylor (April 1970)
- R-71 "A Method of Studying Trapped Particles Behavior in Magnetic Geometries", C.S. Liu and A.Y. Wong (April 1970)
- R-72 "A Note on the Differential Equation $g'' + x^2 g = 0$ ", E.S. Weibel (April 1970)
- R-73 "Plasma Response to a Step Electric Field Greater than the Critical Runaway Field, With and Without an Externally Applied Magnetic Field", J.E. Robin (June 1970)
- R-74 "The UC Mathematical On-Line Systems as a Tool for Teaching Physics", B.D. Fried and R. White (August 1970)
- R-75 "High Frequency Hall Current Instability", K. Lee, C.F. Kennel, J.M. Kindel (August 1970)
- R-76 "Laminar Wave Train Structure of Collisionless Magnetic Slow Shocks", F.V. Coroniti (Sept. 1970)
- R-77 "Field Aligned Current Instabilities in the Topside Ionosphere", J.M. Kindel and C.F. Kennel (Aug. 1970)
- R-78 "Spatial Cyclotron Damping", Craig Olson (September 1970)
- R-79 "Electromagnetic Plasma Wave Propagation Along a Magnetic Field", C.L. Olson (September 1970)
- R-80 "Electron Plasma Waves and Free-Streaming Electron Bursts", H. Ikezi, P.J. Barrett, R.B. White and A.Y. Wong (Nov. 1970)
- R-81 "Relativistic Electron Precipitation During Magnetic Storm Main Phase", R.M. Thorne and C.F. Kennel (Nov. 1970)
- R-82 "A Unified Theory of SAR Arc Formation at the Plasmopause", J.M. Cornwall, F.V. Coroniti and R.M. Thorne (Nov. 1970)
- R-83 "Nonlinear Collisionless Interaction between Electron and Ion Modes in Inhomogeneous Magnetoactive Plasmas", N. Booth (Dec. 1970)
- R-85 "Remote Double Resonance Coupling of Radar Energy to Ionospheric Irregularities", C.F. Kennel (Jan. 1971)
- R-86 "Ion Acoustic Waves in a Multi-ion Plasma", B.D. Fried, R. White, T. Samec (Jan. 1971)
- R-87 "Current-Driven Electrostatic and Electromagnetic Ion Cyclotron Instabilities", D.W. Forslund, C.F. Kennel, J. Kindel (Feb. 1971)

- R-88 "Locating the Magnetospheric Ring Current", C.F. Kennel and Richard Thorne (March, 1971).
- R-89 "Ion Acoustic Instabilities Due to Ions Streaming Across Magnetic Field", P.J. Barrett, R.J. Taylor (March, 1971)
- R-90 "Evolution of Turbulent Electronic Shocks", A.Y. Wong, R. Means (July, 1971)
- R-91 "Density Step Production of Large Amplitude Collisionless Electrostatic Shocks and Solitons", David B. Cohen (June, 1971)
- R-92 "Turbulent Resistivity, Diffusion and Heating", Burton D. Fried, Charles F. Kennel, et al. (June, 1971)
- PPG-93 "Nonlinear Evolution and Saturation of an Unstable Electrostatic Wave", B.D. Fried, C.S. Liu, et al. (August, 1971)
- PPG-94 "Cross-field Current-driven Ion Acoustic Instability", P.J. Barrett, B.D. Fried, C.F. Kennel, J.M. Sellen, and R.J. Taylor (December, 1971)
- R-95 "3-D Velocity Space Diffusion in Beam-Plasma Interaction without Magnetic Field", P.J. Barrett, D. Gresillon and A.Y. Wong (September, 1971)
- PPG-96 "Daytime Auroral Oval Plasma Density and Conductivity Enhancements due to Magnetosheath Electron Precipitation", C.F. Kennel and M.H. Rees (September, 1971)
- PPG-97 "Collisionless Wave-particle Interactions Perpendicular to the Magnetic Field", A.Y. Wong, D.L. Jassby (September, 1971)
- PPG-98 "Magnetospheric Substorms", F.V. Coroniti and C.F. Kennel (September, 1971)
- PPG-99 "Magnetopause Motions, DP-2, and the Growth Phase of Magnetospheric Substorms", F.V. Coroniti and C.F. Kennel (September, 1971)
- PPG-100 "Structure of Ion Acoustic Solitons and Shock Waves in a Two-Component Plasma", R.B. White, B.D. Fried, F.V. Coroniti (September, 1971)
- PPG-101 "Solar Wind Interaction with Lunar Magnetic Field", G. Siscoe (Meteorology Dept.) and Bruce Goldstein (JPL) November, 1971
- PPG-102 "Changes in Magnetospheric Configuration During Substorm Growth Phase", F.V. Coroniti and C.F. Kennel (November, 1971)
- PPG-103 "Trip Report - 1971 Kiev Conference on Plasma Theory and Visits to Lebedev and Kurchatov Institutes", B.D. Fried (October, 1971)
- PPG-104 "Pitch Angle Diffusion of Radiation Belt Electrons within the Plasmasphere", Lawrence R. Lyons, Richard M. Thorne, Charles F. Kennel (January, 1972)
- PPG-105 "Remote Feedback Stabilization of a High-Beta Plasma", Francis F. Chen, Daniel Jassby and M. Marhik, January, 1972